Evaluating the Performance of a Variable Resonance-Frequency Wave-Energy Converter in Irregular Waves[1]

Zhongfei Chen, Binzhen Zhou, Liang Zhang, and Ronald W. Yeung*

College of Shipbuilding Engineering, Harbin Engineering University, Harbin, China
<chenzhongfei@foxmail.com>

University of California at Berkeley, Berkeley, CA 94720-1740
*Correspondence author <rwyeung@berkeley.edu>

HIGHLIGHTS:

- With vectorized and parallel coding, a fast numerical code based on the method of RAO superposition is developed to evaluate the time-domain behaviour of the power absorption.
- The influence of the power-take-off (PTO) parameters on the power-absorption properties of a Variable-Resonance Frequency Wave-Energy Convertor (VRF-WEC) in irregular waves is examined. Multiple ridges are found in the power response in terms of the PTO parameters.

1. INTRODUCTION

To adapt to the constantly varying sea condition, characterized by changing wave frequency and wave height, Chen et al. (2016) developed a new WEC concept: the VRF-WEC, as shown in Fig. 1, which can be designed to have its own resonance frequency changed so as to match the encounter wave frequency, thus enhancing the power absorption capability. Therein, the motion and power responses in the frequency domain in regular waves were reported. The end-stop effects were also researched in irregular waves using the impulse response function (IRF) method in the time domain. It was found that, if properly designed, the end-stop could effectively confine excessive motion and without affecting the power absorption property significantly. These findings allow the present work to examine the power response in irregular waves by RAO superposition method without worrying about the excessive motion, with the understanding that suitable end-stops could be designed. In the present study, only heave degree of freedom (DOF) is being considered. Bachynski et al. (2012) reported that the mooring system just introduced a very low resonance frequency in pitch and surge motion. Thus, the effects of mooring system, which is typically attached to the bottom tip of the VRF-WEC is neglected at this stage of research.

In this study, we use the RAO superposition (RAO-S) method (see e.g. Tom & Yeung, 2014) to calculate the mean power response, and study the influence of the PTO parameters in irregular waves, to be described in the Section 2,.

2. RAO-S METHOD

As illustrated in Fig. 1, the PTO is described by three parameters, namely the internal spring k_m, internal moving mass m and the generator damping force B_g . These parameters, in non-dimensional forms, are given by spring-constant ratio $\bar{s} = k_m / C_3$, mass ratio $\bar{m} = m / M$, and damping ratio $\bar{B}_g = B_g / \lambda_T$, where $C_3 = \rho g \pi a^2$ is the hydrostatic restoring coefficient of the outer floater, and M the total mass of the VRF-WEC system. We followed the notations of Yeung et al (2012) used in similar problems. It was noted that the total damping $\lambda_T = \left(1 + f_{vis}\right)\lambda_{33}$,

[1] Support of the first author's visit at UC Berkeley by the National Natural Science Foundation of China (51409066, 11572094), High-tech Ship Research Projects Sponsored by the Ministry of Industry and Information Technology (MIIT) is acknowledged.

relative to the radiation damping of the outer floater λ_{33}, can be modeled effectively by an experimentally measured coefficient f_{vis} which accounts for separated-flow effects at the bottom edges. Son et al. (2016), has found the viscous coefficient $f_{vis} = 1.725$ for a coaxial-cylinder WEC that employs the patented Berkeley-Wedge shaped bottom (Madhi et al., 2014) (see Fig. 1), for the outer-cylinder bottom, which we will assume in the work below. Recent work of Virey (2016) has found this to be as low as 0.60, which will improve the performance of this concept even more. Nonetheless, to be conservative, we use the former value.

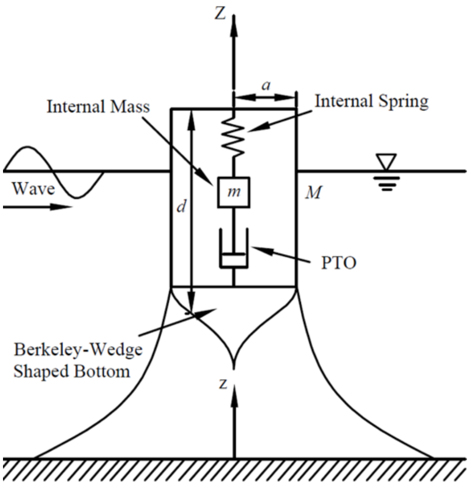

Fig. 1 Schematic of the VRF-WEC concept

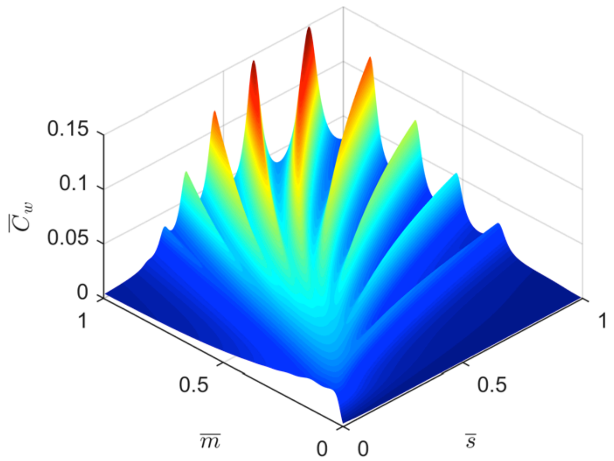

Fig. 2 The non-dimensional capture width for different $\overline{m}$ and $\overline{s}$, with $\overline{B}_g = 3$ and $T_p = 8.5$s

With details given in Chen et al (2016), we would summarize the motion response of the outer cylinder x_3 and the relative position of the internal mass x_{3r}, as shown below, where the inhomogeneous term on the right-hand side represents the vertical wave-exciting force:

$$\begin{bmatrix} M - m + \mu_{33} & 0 \\ 0 & m \end{bmatrix} \begin{Bmatrix} \ddot{x}_3 \\ \ddot{x}_{3m} \end{Bmatrix} + \begin{bmatrix} \lambda_T + B_g & -B_g \\ -B_g & B_g \end{bmatrix} \begin{Bmatrix} \dot{x}_3 \\ \dot{x}_{3m} \end{Bmatrix} + \begin{bmatrix} C_3 + k_m & -k_m \\ -k_m & k_m \end{bmatrix} \begin{Bmatrix} x_3 \\ x_{3m} \end{Bmatrix} = \begin{Bmatrix} f_{e3} \\ 0 \end{Bmatrix} \tag{1}$$

and the hydrodynamic coefficients were obtained from Yeung (1981). In this study, a fairly standard random irregular waves are generated by the ISSC wave spectrum for fully-developed seas. With the aforementioned RAO-S method, the non-dimensional capture width, relative to the diameter *2a* of the VRF-WEC is written as:

$$\overline{C}_w = \frac{P_m}{2a \cdot P_w} = \frac{\dfrac{B_g}{T}\displaystyle\int_0^T \left(\Re \left\{ \sum_{j=1}^{N} -i\omega_j \left| RAO_r\left(\omega_j\right) \right| \left| A_j\left(\omega\right) \right| e^{-i\left(\omega_j t + \varphi_j + \varepsilon_j\right)} \right\} \right)^2 dt}{2a \cdot \displaystyle\sum_{j=1}^{N} \tfrac{1}{2} \rho g \left| A_j\left(\omega\right) \right|^2 V_{g,j}} \tag{2}$$

where P_m is the mean power absorption of the VRF-WEC, over a long duration of *T,* and P_w is the wave-energy transportation rate per unit crest width. $\left|A_j\left(\omega\right)\right|$ is the wave amplitude of each component. RAO_r is the RAO of the relative motion x_{3r}, and $V_{g,j}$ is the group velocity of each wave component. Equations for the relative-motion RAO of can be found in Chen et al. (2016).

The RAO-S method is based on the linear hypothesis. It was fount we that the results with the IRF method, also a linear method, differ by less than 1%, with properly vectorized and parallel coding (instead of sequentially circulation coding) using MATLAB. As expected, the RAO-S can be thousands times faster than the IRF method in terms such type of computations. For a given wave climate (certain T_p and H_s), results for $T = 100{,}000T_p$ and $N = 100$ in Eqn (2) and those with $T = 200{,}000T_p$ and $N = 200$ are also obtained for comparison. The difference between the two sets of run parameters is less than 0.01%. The calculation time is just 0.2~0.3s with vectorized coding for one wave climate (4 cores Intel i7 CPU, 3.4GHz). Even so, to obtain acceptable resolution, Fig. 2 which consists of 10 thousand points still needed 40~50 mins time of parallel computations.

3. EFFECTS OF PTO PARAMETERS ON PERFORMANCE

For the VRF-WEC, the power response is a function of three types of parameters, namely geometric (radius a, draft d, and water depth h), mechanical (mass ratio $\overline{m}$, spring ratio $\overline{s}$, and damping ratio $\overline{B}_g$), wave climate (wave peak period T_p, and significant wave height H_s). The purpose of this abstract is to study the influence of the mechanical parameters on the power response for given geometry of VRF-WEC in a given wave condition. The geometric parameters are taken as radius $a = 2.2\text{m}$, draft $d = 5.5\text{m}$, and water depth $h = 60.0\text{m}$, as well as the wave climate parameter set as wave peak period $T_p = 8.5\text{s}$, significant wave height $H_s = 1.0\text{m}$.

Chen et al., (2016) found that the VRF-WEC has two resonance frequencies Ω_1 and Ω_2 which were mainly determined by $\overline{m}$ and $\overline{s}$ only, while the value of $\overline{B}_g$ only affects the response amplitude when $\overline{B}_g$ is small. If we set $\overline{B}_g$ to be a constant and varying $\overline{m}$ and $\overline{s}$ to calculate the non-dimensional capture width $\overline{C}_w$ using regular waves, only one ridge (at which the Ω_1 or Ω_2 matches the wave-encountering frequency) could be found (similar to what is shown in Fig. 2 but with only a single ridge). This ridge represents the band around which performance is of energy extraction is excellent. However, with irregular waves as input, multiple ridges are found, as shown in Fig. 2. Furthermore, if we change the $\overline{m}$ and $\overline{s}$ to match Ω_1 with the peak frequency of encounter in irregular waves, the ridge line does not correspond to a specific $\overline{m}$ and $\overline{s}$ value. Consequently, the optimization procedure that Chen et al. (2016) had used in the regular-wave analysis may not be suitable for treating irregular waves. A new optimization method is needed to find the optimal PTO parameter with relative small amount of numerical calculation cost. Of interest is the observation that the locations of ridges do not change much, but the ridges become "smoother" as $\overline{B}_g$ increases. This phenomenon follows the same characteristics as in regular wave analysis. If $\overline{B}_g$ is very large ($\overline{B}_g \geq 10$ for this example), these multiple ridges converge into one peak. The reason why the power response of VRF-WEC have multiple ridges even when the wave spectrum is smooth is unknown. However, this type of non-convex function with multiple ridges makes it difficult to find the global peak without a massive amount of searching.

Fortunately, for given $\overline{m}$ and $\overline{s}$, the $\overline{C}_w$ curve has only one peak with respect to $\overline{B}_g$. If we define the corresponding $\overline{B}_g$ as optimal $\overline{B}_{g\_opt}$ for given $\overline{m}$ and $\overline{s}$, $\overline{B}_{g\_opt}$ can be found using simple searching method by 3~5s calculation for each $\bar{m}$ and $\bar{s}$ combination. Thus, Fig. 3 presents the variation of the non-dimensional capture width $\bar{C}_w$ and the corresponding $\bar{B}_{g\_opt}$ is shown in Fig. 4. Fig. 4 illustrates that the $\bar{C}_w$ response still have multiple sharp ridges. Generally,

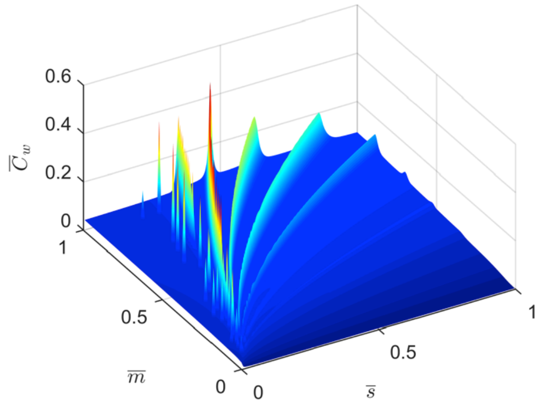

Fig. 3 The non-dimensional capture width $\bar{C}_w$ with optimal $\bar{B}_g$ for different $\bar{m}$ and $\bar{s}$ at $T_p = 8.5$s

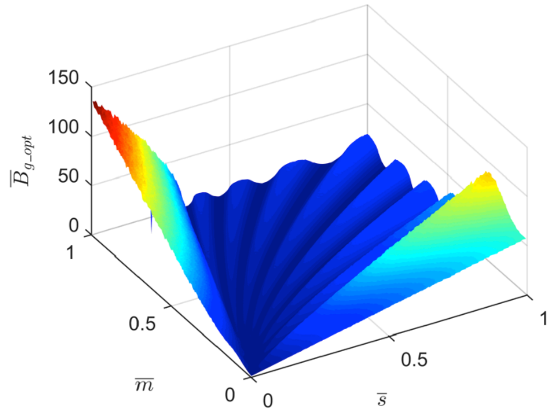

Fig. 4 The optimal $\bar{B}_g$ for different $\bar{m}$ and $\bar{s}$ at $T_p = 8.5$s

$\bar{C}_w$ seems to increase with increasing $\bar{m}$ and $\bar{s}$. A VRF-WEC can reach $\bar{C}_w \approx 0.5$ without using any real-time control strategy in irregular waves. The sharp peaks at small $\bar{s}$ is because the resolution of $\bar{m}$ and $\bar{s}$ is not adequate. However, for now, Fig. 3 and Fig. 4 are the best solution we can do with 40 thousand points and with 37h of calculations. Of course, the process can be made faster by using a more powerful computer or searching algorithm, including genetic algorithm, particle swarm optimization, which we can report in the near future.

4. SUMMARY REMARKS

With vectorized and parallel coding, the RAO-S method can be thousand times faster than the IRF method for evaluating the performance of a VRF-WEC in irregular waves. Based on this fast method, a PTO parametric study is presented. In the power-response, multiple ridges of high-power performance are found in the ($\bar{m}$ - $\bar{s}$) space at certain $\bar{B}_g$. $\bar{B}_g$ affects only the amplitudes of the ridges and has little influence on the location of the ridges when $\bar{B}_g$ is relatively small. This fast numerical optimization will help to determine the appropriate PTO parameters in irregular waves.

References

Bachynski, E. E., Young, Y. L., and Yeung R. W., Analysis and optimization of a tethered wave energy converter in irregular waves. *Renewable Energy,* 2012;48:133-145.

Chen, Z., Zhang, L., and Yeung R W., "Analysis and Optimization of a Dual Mass-Spring-Damper (DMSD) Wave-Energy Converter with Variable Resonance-Frequency Capability", Applied Ocean Research 2016; (submitted).

Madhi, F., Sinclair, M. E., and Yeung, R. W., "The "Berkeley Wedge": an asymmetrical energy-capturing floating breakwater of high performance", *J. Marine Systems and Ocean Technology (MS&OT),* 2014, vol. 9, no. 1, pp 5-16. US Provisional Patent No. 61/883,274; USPTO # 9,416,766 (http://pdfpiw.uspto.gov/.piw?Docid=09416766)

Tom, N. and Yeung, R. W., "Non-Linear Model Predictive Control Applied to a Generic Ocean-Wave Energy Extractor," *Journal Offshore Mechanics and Arctic Engineering,* Vol. 136, 04190-1, November 2014.

Son D., Belissen V., and Yeung R. W., "Performance validation and optimization of a dual coaxial-cylinder ocean-wave energy extractor", *Renewable Energy,* 2016;92:192-201.

Viray, L. "Design and Evaluation of a Variable Resonance-Frequency Wave-Energy Converter", MS Thesis, December 2016, University of California at Berkeley

Yeung, R. W.,"Added Mass and Damping of a Vertical Cylinder in Finite-Depth Waters", *Appl Ocean Res.* 3 (3):119-33.